The EMBO Journal vol.14 no.8 pp.1690–1696, 1995

Structure of the major antigenic loop of foot-and-mouth disease virus complexed with a neutralizing antibody: direct involvement of the Arg-Gly-Asp motif in the interaction

Nuria Verdaguer, Mauricio G.Mateu[1], David Andreu[2], Ernest Giralt[2], Esteban Domingo[1] and Ignasi Fita[3]

Departament d'Enginyeria Química, Universitat Politécnica de Catalunya, 08028 Barcelona, [1]Centro de Biología Molecular 'Severo Ochoa' (CSIC-UAM), Universidad Autónoma de Madrid, 28049 Madrid and [2]Departament de Química Orgànica, Universitat de Barcelona, 08028 Barcelona, Spain

[3]Corresponding author

Communicated by E.Domingo

The crystal structure of a synthetic peptide representing the major antigenic loop of foot-and-mouth disease virus (FMDV), complexed with the Fab fragment of a neutralizing monoclonal antibody raised against the virus, has been determined at 2.8 Å resolution. The peptide shows a high degree of internal structure with a nearly cyclic conformation. The conserved Arg-Gly-Asp motif, involved in the viral attachment of aphtoviruses to cells, participates directly in the interaction with several complementarity determining regions of the antibody molecule. The Arg-Gly-Asp triplet shows the same open turn conformation found in the reduced form of FMDV of another serotype and also in integrin binding proteins. The observed interactions provide a molecular interpretation of the amino acid replacements observed to occur in mutants resistant to neutralization by this antibody. The structure also suggests a number of restrictions to variation within the epitope which are imposed to keep the Arg-Gly-Asp motif in its functional conformation.

Key words: antigen–antibody complex/foot-and-mouth disease virus/RGD receptor/viral epitope

Introduction

A hallmark of RNA viruses is their population complexity, rapid antigenic variation and ability to escape from neutralization by antibodies (Steinhauer and Holland, 1987; Holland *et al.*, 1992). The understanding of mechanisms of viral neutralization (Dimmock, 1993) and of escape from antibody recognition requires a detailed knowledge of viral antigen–antibody interactions at the molecular level. Such critical information is at present very limited (Davies *et al.*, 1990; Laver *et al.*, 1990; Rini *et al.*, 1992; Tulip *et al.*, 1992; Smith *et al.*, 1993; Ghiara *et al.*, 1994; Tormo *et al.*, 1994).

Foot-and-mouth disease virus (FMDV) is a particularly relevant representative of the highly variable RNA viruses, since it is the economically most important animal pathogen worldwide (Bachrach, 1968; Pereira, 1981; Domingo *et al.*, 1990). The disease FMD can be controlled by the slaughter of affected animals or by regular vaccination in enzootic areas. However, the effectiveness of current inactivated virus vaccines and the development of new synthetic vaccines against FMD have been hampered by the extensive antigenic variation of the virus. Seven distinct serotypes (A, O, C, Asia1, SAT1, SAT2 and SAT3) and multiple variants within each serotype have been described. A major, highly variable antigenic site (site A) of FMDV involved in virus neutralization (Bittle *et al.*, 1982; Pfaff *et al.*, 1982; Strohmaier *et al.*, 1982) is located within the G–H loop of capsid protein VP1 (Acharya *et al.*, 1989; Figure 1). This capsid segment, either as a peptide or as part of fusion proteins, has been incorporated in a number of synthetic vaccine formulations against FMD (Di Marchi *et al.*, 1986; Clarke *et al.*, 1987; Brown, 1992). However, protection has not been always complete and no synthetic vaccine against this disease is available at present. The G–H loop of VP1 includes a conserved Arg-Gly-Asp (RGD) motif which mediates attachment to cells and virus infectivity (Fox *et al.*, 1989; Surovoi *et al.*, 1989; Baxt and Becker, 1990; Mason *et al.*, 1994). The conformation of the G–H loop could not be defined in any of the several crystal structures determined for native FMDVs (including isolates O_1BFS of serotype O and C-S8c1 of serotype C; Acharya *et al.*, 1989; Parry *et al.*, 1990; Lea *et al.*, 1994). However, for this loop a structure was defined upon the reduction of a disulfide bridge on the capsid of FMDV type O, a treatment which did not result in loss of infectivity (Logan *et al.*, 1993). In type C virus the loop appeared as disordered in the X-ray diffraction analysis, despite the disulfide bond being absent in this serotype (Lea *et al.*, 1994).

Multiple naturally occurring substitutions at two hypervariable segments within the G–H loop of FMDV (Figure 1) led to significant antigenic differences among variant viruses of this serotype. In addition, single amino acid replacements at any one of a few critical positions did affect the antigenic specificity of this site severely, and this has been documented with both field viruses and laboratory variants (Mateu *et al.*, 1989, 1990, 1994; Martínez *et al.*, 1991a; Hernández *et al.*, 1992; Borrego *et al.*, 1993). Such antigenic differences can be faithfully mimicked with synthetic peptides which included the relevant substitutions (Rowlands *et al.*, 1983; Mateu *et al.*, 1989, 1992; Carreño *et al.*, 1992). The interpretation of the effect of amino acid replacements in viral neutralization can be aided greatly by structural information of antigen–antibody complexes. In this report we describe the crystal structure of a 15 amino acid peptide A15 (sequence YTASARGDLAHTTT-NH_2; Figure 1) which represents antigenic site A of FMDV C-S8c1 complexed with the Fab fragment of a strongly neutralizing monoclonal antibody (mAb SD6). This antibody was elicited against the virus and recognizes a continuous epitope

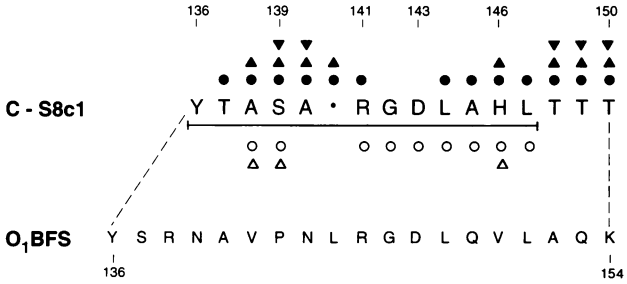

Fig. 1. Amino acid sequence of peptide A15 (antigenic site A) of FMDV C-S8c1. The dot in the sequence indicates the absence of one amino acid residue relative to some other type C viruses (Martínez *et al.*, 1991a). The sequence of the equivalent segment from FMDV O_1BFS (Logan *et al.*, 1993) is given below for comparison. Antigenic site A of FMDV C-S8c1 was mapped between residues 136 and 150 of VP1 using overlapping peptides, nine neutralizing antivirus mAbs and 13 sera from convalescent or vaccinated swine (Mateu *et al.*, 1989, 1990, 1992 and unpublished results). These mAbs defined continuous epitopes, in that they reacted with VP1 and synthetic peptides almost as efficiently as with virions (Mateu *et al.*, 1989, 1990). The mAb SD6 epitope is underlined. (○) Residues at which substitutions affected recognition of the virus or peptide by mAb SD6. (△) Residues substituted in 70 SD6-resistant mutants of C-S8c1 (Mateu *et al.*, 1989; Carrillo *et al.*, 1990). Ala138 was replaced by Asp or by Pro; Ser139 by Gly, Ile, Asn or Arg; and His146 by Arg. Above the sequence: (●) variable positions in 50 type C field viruses sequenced. Segments 141–143 and 144–147 are highly conserved (0.006 and 0.10 substitutions per residue, respectively, relative to the consensus); segments 137–140 and 148–150 are more variable (0.32 and 0.31 substitutions per residue, respectively; Martínez *et al.*, 1991a). (▲) Residues replaced in 97 laboratory mutants (89 of them derived from C-S8c1) selected with monoclonal (Mateu *et al.*, 1989, 1990; Carrillo *et al.*, 1990; Hernández *et al.*, 1992 and unpublished results) or polyclonal (Borrego *et al.*, 1993) antibodies. (▼) Residues replaced in mutants obtained in 25 independent passages of FMDV type C in cell culture in the absence of immune pressure (Díez *et al.*, 1989; Martínez *et al.*, 1991b; Borrego *et al.*, 1993; Domingo *et al.*, 1993; A.Holgin, J.Hernandez, M.G.Mateu and E.Domingo, unpublished results).

which has been characterized previously (Figure 1). The structure reveals that the ubiquitous RGD motif participates directly in the interaction and provides new insights into the molecular basis of the antigenic variation of FMDV.

Results

Overall structure of the FMDV peptide–Fab complex

The four Fab–peptide complexes located in the asymmetric unit of the crystal were very accurately related by non-crystallographic symmetry. The averaged r.m.s. between variable and constant modules of the four complexes were 0.32 and 0.28 Å, respectively. The structure of each complex comprises 438 residues from the Fab fragment (218 residues from the light chain and 220 residues from the heavy chain) and the 15 peptide residues. The final averaged electron density map allowed the positioning with confidence of most amino acid side chains in the complex. In particular, density is clearly defined around the antigen binding site. Thus, all residues in the peptide could be unambiguously positioned (Figure 2). All peptide and Fab residues are inside or near the energetically allowed regions in the Ramachandran diagram (see Figure 3 for the peptide residues).

A structure for the G–H loop of FMDV complexed to antibody

The FMDV peptide complexed to anti-virus Fab SD6 depicts a compact folded conformation with a high degree of internal structure (Figure 4A and B). A short helical segment and three hydrogen bonded turns are observed in the complexed peptide (Figure 4A). The structure is stabilized further by four hydrogen bonds formed between

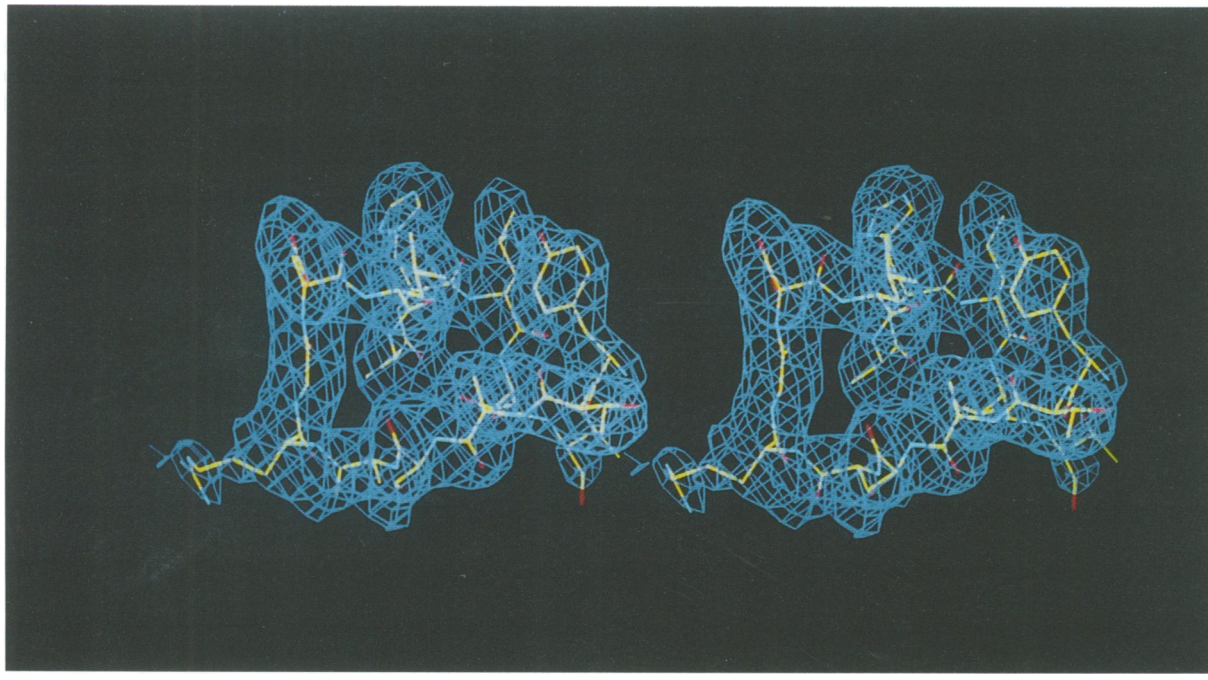

Fig. 2. Stereoview of an averaged (F_o – F_c) omit map (in blue) of the peptide at 2.8 Å resolution. The peptide model placed inside the density is also shown for clarity. Tyr136 is shown on the right and the RGD motif is on the left-hand side of the figure. The weakest density corresponds to the side chain from Arg141 and the C-terminal Thr149 and Thr150. The figure was displayed using the program TURBO (Rousel and Cambillau, 1991) on an Indigo Silicon Graphics workstation.

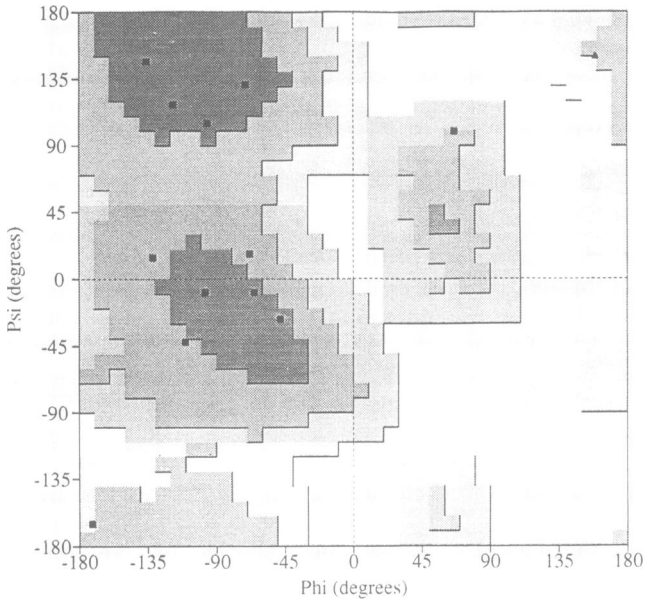

Fig. 3. Ramachandran plot of the bound peptide obtained with the program PROCHECK (Laskowski *et al.*, 1994). The N-terminal residues (from Tyr136 to Ala140) are clustered in the β-region, while most amino acids in the C-terminal segment (from Asp143) are inside the helical regions.

main-chain and side-chain atoms (Figure 4A). The N- and C-terminal residues interact with each other, giving an almost cyclic character to the peptide structure. The RGD motif appears in an open turn conformation; the side chains from Arg141 and Asp143 of the RGD are located far apart (distance between C_β atoms of 9.5 Å), with no possible direct interaction between them. A least squares superposition of C_α atoms from the RGD residues in the type C peptide with the equivalent residues in the reduced type O virus gave an average r.m.s. deviation of only 0.23 Å. The orientations of the side chains are also coincident, with a r.m.s. deviation, when C_β atoms are considered, of 0.32 Å (Figure 4C). The conformation of the RGD in the type C peptide is thus extremely similar to that found in the G–H loop of reduced type O FMDV (Logan *et al.*, 1993; Figure 4C) and in integrin binding proteins involved in promoting or inhibiting cell adhesion (Wistow *et al.*, 1983; Ruoslahti, 1988; Hynes, 1992; Leahy *et al.*, 1992; Lazarus *et al.*, 1993; Krezel *et al.*, 1994). The helical segment in the peptide structure involves Asp143 to Leu147. In the G–H loop of reduced type O FMDV, a helix is also initiated at the equivalent position, and its direction is essentially coincident with that in the peptide. The helical structure in the peptide could be stabilized by the presence of a hydrogen bond between atom $N_\delta 1$ from His146 and the main-chain oxygen atom from Asp143. The structural similarities between the G–H loop of reduced type O virus and the type C peptide strongly suggest that the conformation of the RGD triplet and of the adjacent helical segment are conserved features of this loop in aphtoviruses.

The aromatic ring of Tyr136, a residue absolutely conserved in all FMDVs sequenced to date, interacts strongly with the side chain from Leu147, which is highly conserved in type C viruses and also in other FMDV serotypes (Martínez *et al.*, 1991a; Domingo *et al.*, 1992). The arrangement of Tyr136 and of hypervariable residues 137–140 in the N-terminal region and 148–150 in the C-terminal region of the peptide differs considerably from that in the type O loop. This is not surprising given the low level of amino acid identity (including an insertion of four residues in type O) between the two viruses within these variable segments (Figure 1).

The FMDV peptide–antibody interactions include direct participation of the RGD motif

The arrangement of the complementarity determining regions (CDRs) in mAb SD6 creates a cavity occupied by the peptide in the complex (Figure 5A). The contact surface areas calculated using the program MS (Connolly, 1983; Figure 6), with a 1.7 Å probe radius and standard van der Waals radii (Case and Karplus, 1979), are 430 $Å^2$ on the peptide and 422 $Å^2$ on the Fab. The paratope of mAb SD6, elicited against the virion, is concave, as found generally for antipeptide antibodies, and it differs from the essentially planar paratopes found for other antiprotein antibodies (Wilson and Stanfield, 1993; Webster *et al.*, 1994). A concave paratope has been described previously for a neutralizing mAb, elicited against human rhinovirus, which also recognizes a continuous epitope (Tormo *et al.*, 1994). These observations suggest that large protruding loops in protein antigens can behave as true native continuous epitopes, recognized by antibodies with concave paratopes to maximize the contact area.

The Fab SD6 surface in direct contact with the peptide comprises four of the six CDR loops (L1, L3, H2 and H3; Figure 5). Fourteen hydrogen bonds between the F(ab) and the peptide (Table I), three of them with ionic character, emphasize that polar interactions are important for specific recognition in this antigen–antibody complex (Figure 5). Previous studies (Mateu *et al.*, 1989; Figure 1) have shown that only three VP1 residues (Ala138, Ser139 and His146) appeared substituted by a restricted subset of amino acids in >70 mAb SD6-resistant mutants of FMDV C-S8c1 selected from independent mutational events (on FMDV C-S8c1 preparations grown from different viral plaques). Ala138 buries 75% (25 $Å^2$) of its surface area upon interaction with the mAb (Figure 6). Ser139 is in direct contact with both CDR L1 and CDR L3, forming two hydrogen bonds with Ser31 (CDR L1) and Asn96 (CDR L3). His146 is hydrogen bonded to Ser52, Ser53 and Tyr59 from the CDR H2 loop. The strong involvement of Ala138, Ser139 and His146 in the recognition by the antibody explains the sensitivity to substitutions at these positions. However, in addition to these three residues, immunochemical results (Mateu *et al.*, 1989; Martínez *et al.*, 1991a; Novella *et al.*, 1993; Figure 1) indicated that the highly conserved VP1 amino acids 141–143 (the RGD motif), Ala145 and Leu147 were involved, directly or indirectly, in recognition by mAb SD6. The structure shows that all of these amino acids are in direct contact with the antibody (Table I and Figure 6). Interactions involving the RGD motif are highlighted in Figure 5. The carboxylate group of Asp143 forms a hydrogen bond with O_γ in Thr50 (from CDR H2) and a double hydrogen bond with Arg99 (from CDR H3). Asp143 also has non-polar interactions with side chains of Val98 and Leu100 (from CDR L3). Gly142 contacts by >80% of its surface with SD6. Both main and

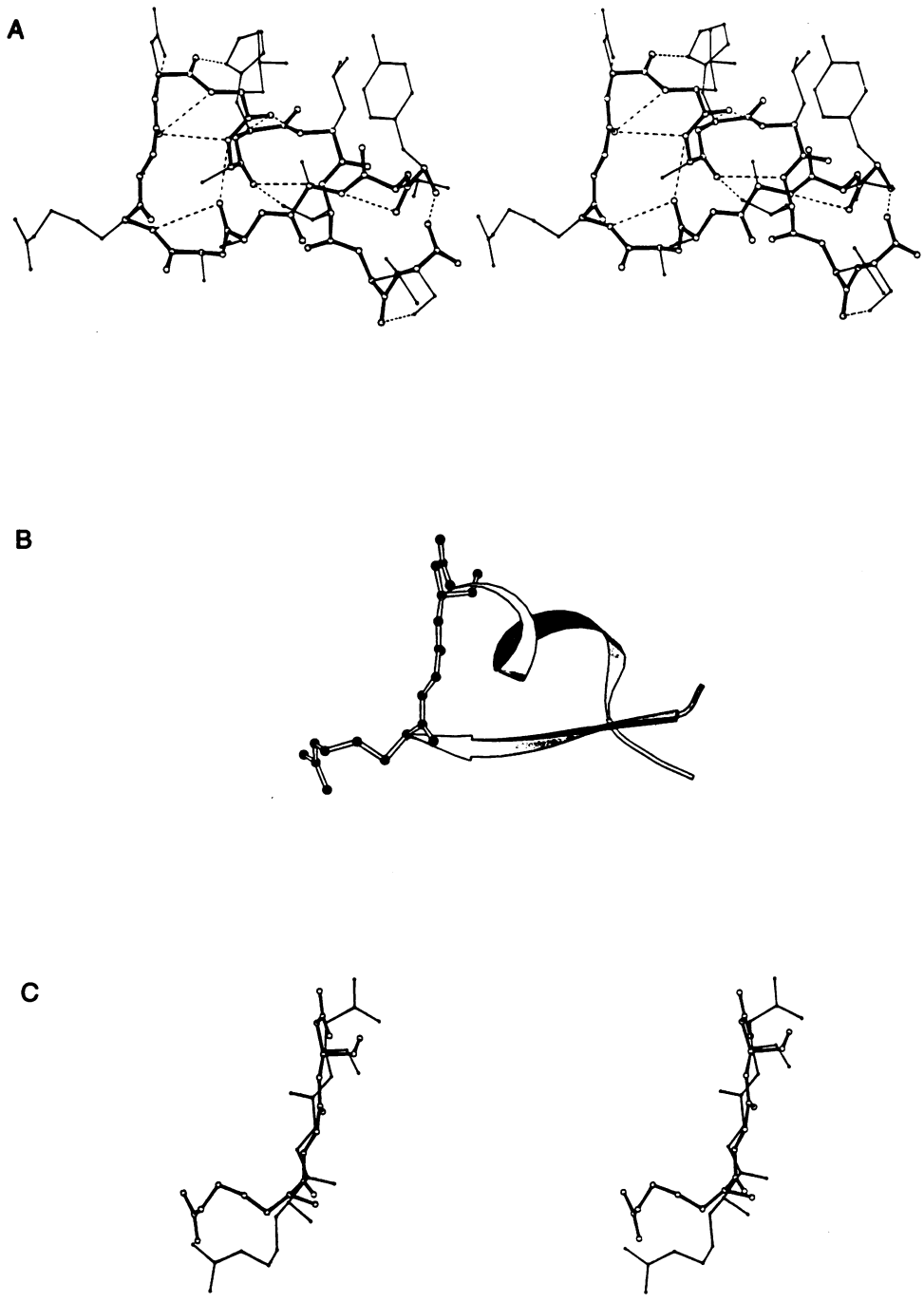

Fig. 4. (**A**) Stereoplot of the antigenic peptide. Hydrogen bonds are indicated by discontinuous lines. The main chain is highlighted with thicker bonds. (**B**) Molscript diagram (Kraulis, 1991) of the peptide structure. The RGD motif is shown in detail. (**C**) Superimposition of the RGD motif in the FMDV C-S8c1 peptide (thicker lines) with the equivalent residues in the G–H loop structure of reduced FMDV O_1BFS (thin lines).

side chains of Arg141 are hydrogen bonded with Glu97 (CDRL3), which remains partially exposed to solvent (Figure 6).

Discussion

The determination of the 3-D structure of complexes between viral antigens and antibody molecules is instrumental in defining the molecular basis of the antigenic variation of viruses. In the antigen–antibody complex reported here for FMDV of serotype C (clone C-S8c1), it is apparent that, due to the number and specificity of the interactions observed, even chemically conservative substitutions of Asp143 and, to a lesser extent, of Arg141 and Gly142 are expected to be disruptive. This is in agreement with previous studies using substituted peptides which showed that the replacement of Asp143 abolished binding to mAb SD6 and to most other mAbs and polyclonal antibodies tested. Also, replacements of Arg141 or Gly142 interfered with antibody binding (Novella *et al.*, 1993). Our results, along with the previous evidence of the involvement of RGD in the recognition of the cellular

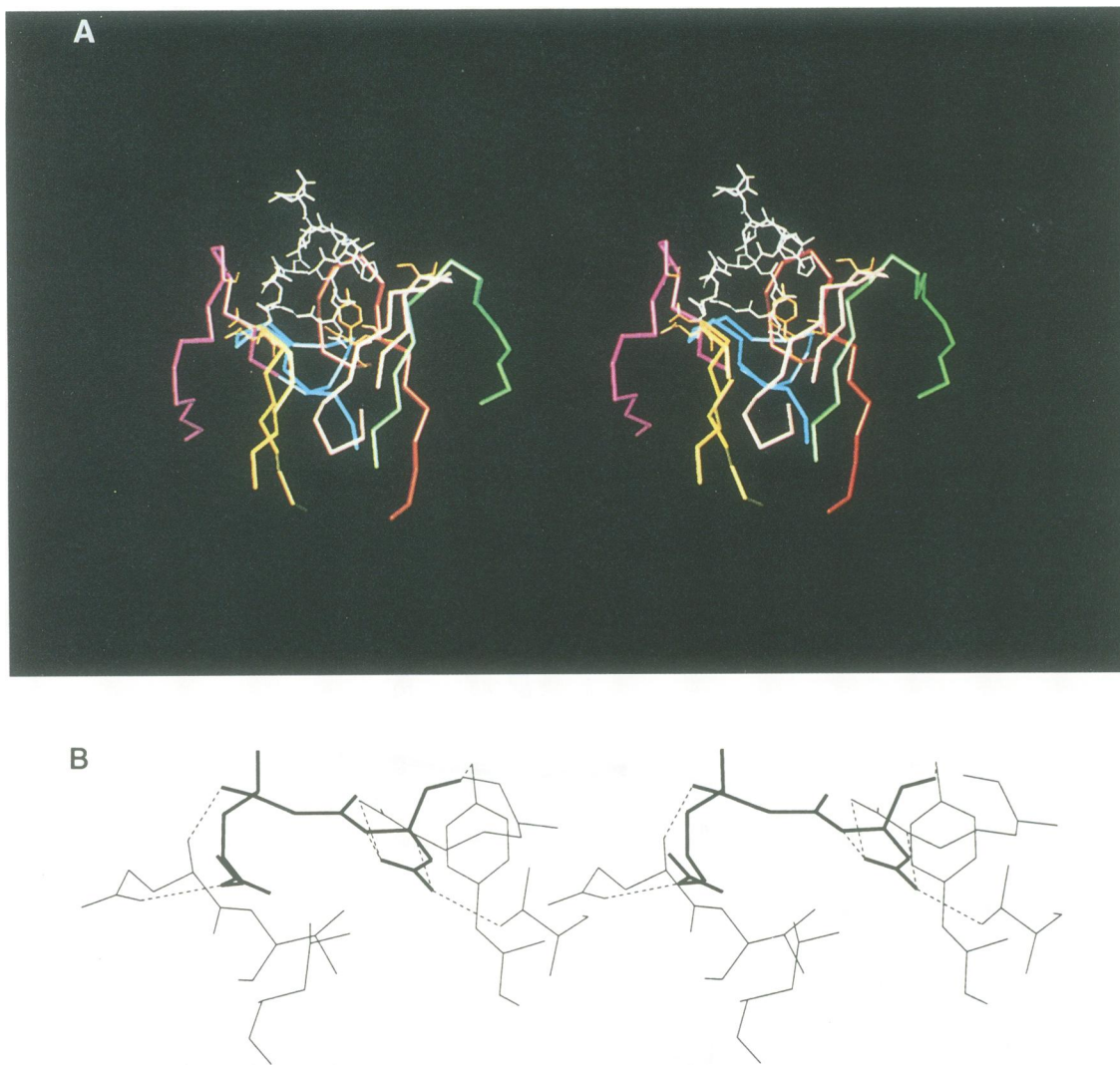

Fig. 5. Stereoviews of the peptide–Fab interactions. (Note that, for clarity, the orientation used differs from that in Figures 2 and 4). (**A**) Binding pocket of the Fab SD6–peptide complex. The main chains of the six CDRs are shown in different colors. Light chain CDRs are on the left (CDRL1, violet; CDRL2, blue; CDRL3, yellow) and heavy chain CDRs are on the right (CDRH1, green; CDRH2, pink; CDRH3, red). Fab residues, hydrogen bonded with the peptide, are depicted in brown. The whole peptide is shown in white. (**B**) Detail of interactions involving the RGD motif (amino acids Arg141–Gly142–Asp143 represented with thick lines). All Fab residues in direct contact with the motif are shown (thinner lines).

receptor (Fox *et al.*, 1989; Mason *et al.*, 1994), suggest that the conserved RGD in FMDV has a dual function, serving both in cell recognition and attachment and as an integral part of a viral epitope. Severe restrictions to variation of this motif must be in operation despite it being a critical part of a neutralization epitope, because interaction with the cell receptor is an essential step in the viral life cycle. For other picornaviruses, Rossmann and colleagues formulated the 'canyon hypothesis' (Rossmann, 1989; Rossmann *et al.*, 1985), according to which the receptor recognition sites were located at a canyon or pit rather than on an exposed capsid domain; this would shield the critical residues from immune attack because antibody molecules would not be able to reach the bottom of the canyon. Such a location has been confirmed for human rhinovirus by cryoelectron microscopy studies of virus–receptor complexes (Olson *et al.*, 1993), thus supporting the canyon hypothesis. In contrast, the structure of the FMDV loop–antibody complex clearly indicates that aphtoviruses do not shield the RGD motif from antibody attack. Rather, the current evidence points to the continuous action of negative selection (the elimination of mutants with substitutions at the RGD or critical surrounding amino acids) to maintain amino acid sequences needed for virus infectivity. Despite its critical role in recognition by mAb SD6, and possibly by most antibodies directed to site A (Novella *et al.*, 1993; M.G. Mateu *et al.*, unpublished results), almost no substitution at the RGD has been observed among many antigenic variants or escape mutants of FMDV (Figure 1).

VP1 residues 144–147, adjacent to the RGD sequence, adopt a helical path in the structure of the FMDV loop and are highly conserved in serotype C (Martínez *et al.*, 1991a; Figure 1). Such conservation may reflect the need to maintain the helical structure which, in turn, may be required to keep the RGD motif in a functional conformation. The few replacements found within the helical segment critically affect the interaction with most anti-

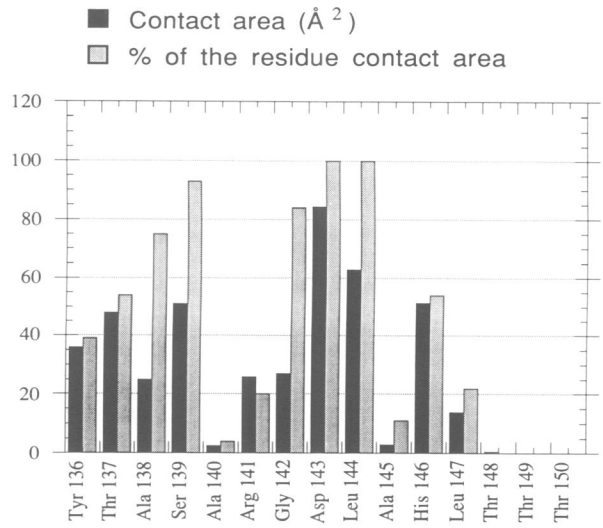

Fig. 6. Buried area expressed in Å^2 and percentage of residue contact area for the FMDV C-S8c1 peptide in the complex.

Table I. Hydrogen bonds between the peptide and the Fab fragment in the complex

FMDV C-S8c1 peptide	SD6 Fab fragment	Distance (Å)
Tyr136 O_η	Glu100 $O_\varepsilon 2$ (H3)	2.62
Tyr136 O_η	Gly103 N (H3)	3.27
Thr137 O	Asp104 N (H3)	2.70
Ser139 O_γ	Ser31 O_γ (L1)	3.22
Ser139 O_γ	Asn96 $O_\delta 1$ (L3)	3.32
Arg141 O	Glu97 N (L3)	2.65
Arg141 N_ε	Glu97 $O_\varepsilon 1$ (L3)	3.12
Asp143 O	Tyr59 O_η (H2)	3.40
Asp143 $O_\delta 1$	Arg99 $N_\eta 2$ (H3)	3.31
Asp143 $O_\delta 2$	Arg99 $N_\eta 2$ (H3)	3.20
Asp143 $O_\delta 2$	Thr50 $O_\gamma 1$ (H2)	2.65
His146 $N_\delta 1$	Tyr59 O_η (H2)	2.77
His146 $N_\delta 2$	Ser52 O_γ (H2)	3.27
His146 $N_\delta 2$	Ser53 O_γ (H2)	2.82

bodies, leading to antigenically highly divergent type C viruses (Gebauer *et al.*, 1988; Mateu *et al.*, 1990, 1992; Martínez *et al.*, 1991a; Hernández *et al.*, 1992; Borrego *et al.*, 1993).

This study, as well as others (Compton *et al.*, 1991; Reynolds *et al.*, 1991; Smith *et al.*, 1993; Lea *et al.*, 1994), suggests that the characterization of contact and functional epitopes by mapping amino acid substitutions in mAb-resistant mutants may be limited by severe constraints to variation, even in highly variable RNA viruses. The results also support the view that the variation of FMDV, and perhaps other picornaviruses, is mediated to a considerable extent by repeated replacements at only a few positions which are tolerant to change within antigenic sites (Lea *et al.*, 1994; Mateu *et al.*, 1994). The observed interactions between the RGD and the antibody provide a molecular interpretation of viral neutralization by antibodies directed to site A of FMDV by direct blocking of the interaction with the cell receptor (Baxt *et al.*, 1984). Finally, the structure of the site A peptide-neutralizing antibody complex has a number of implications for FMD control. In particular, the nearly cyclic nature of this loop suggests that a simple cyclization, which may adequately restrict the conformations of the linear peptide, may improve it as a synthetic vaccine immunogen.

Materials and methods

Crystallization and data collection

The production and purification of mAb SD6 (Mateu *et al.*, 1987) and its Fab fragment have been described previously (Verdaguer *et al.*, 1994). Crystals of the Fab SD6–peptide A15 complex were obtained with 6 µl hanging droplets initially containing 7.6 mg/ml Fab, 1 mg/ml peptide, 8% PEG 4K with 0.1 M potassium phosphate (pH 6.5), and equilibrated at room temperature against a reservoir containing 18% PEG equally buffered. The crystals were triclinic, space group P1 and unit cell parameters a = 56.2 Å, b = 60.6 Å, c = 143.2 Å, α = 90.1°, β = 95.4°, γ = 92.7°, containing four complexes per asymmetric unit, which would correspond to a specific volume solvent content of 49%. The X-ray diffraction data were collected to 2.8 Å resolution using an Image Plate (MarResearch) area detector in a GX 21 rotating anode generator and were reduced with the MARXDS program package (Kabsch, 1988). A dataset obtained from five crystals was 70.1% complete to 2.8 Å resolution (87.2% to 3.2 Å resolution), with a merging R.value of 0.11 based on intensities.

Structure solution and refinement

The structure was determined by molecular replacement using the AMoRe package (Navaza, 1994). The starting models were taken from the structure of the uncomplexed Fab fragment of antibody SD6 which had been determined previously with a crystallographic agreement factor of 18.6% for 16 738 reflections in the resolution shell (7.0–2.5 Å; N.Verdaguer *et al.*, manuscript in preparation). The correctly oriented and positioned models were subjected to rigid body refinement with the program XPLOR (Brünger, 1992). During the final cycles, the variable heavy, variable light, constant heavy and constant light domains were allowed to move as four separate bodies. The resulting R factor was 36.5% in the resolution range 15.0–3.5 Å. At this stage $2F_o - F_c$ and $F_o - F_c$ electron density maps clearly showed extra density corresponding to the oligopeptide occupying the antigen binding site. Some conformational rearrangements in the CDRs of the antibody were also visible, especially in the hypervariable loop H3. After omitting all the residues in the variable regions, positional refinement was started. Cycles of automatic refinement were alternated with manual model rebuilding in an iterative process that gave the final model with an agreement R factor of 18.2% for 30 908 reflections, with $F_o > 2\sigma$ (F_o) in the resolution shell 8.0–2.8 Å. The r.m.s. deviations from ideality on bond lengths and angles are 0.022 Å and 3.1°, respectively.

The presence of non-crystallographic symmetry was used both as a restraint during refinement with the XPLOR program and to improve the quality of the maps. Cycles of electron density averaging and solvent flattening were applied along with the PHASES package (Furey, 1993). Density corresponding to variable and constant modules had to be averaged separately. The model building was always carried out using averaged maps. The final agreement R factor in the electron density manipulation was 17.7% and the correlation coefficient was 96% (Rossmann *et al.*, 1985).

Acknowledgements

We thank X.Roig and I.S.Novella for peptide synthesis and B.Borrego for help in the production of mAb SD6. Research at the Universitat Politécnica was supported by grants PB92-0707 and PB90-0605. Work at the CBM was supported by grants BP91-0051-CO2-01 and BIO91-1531-CE from The CE and Fundación Ramón Areces. Work at the University of Barcelona was supported by grant PB91-0266 from the DGICYT.

References

Acharya,R., Fry,E., Stuart,D., Fox,G., Rowlands,D. and Brown,F. (1989) *Nature*, **337**, 709–716.
Bachrach,H. (1968) *Annu. Rev. Microbiol.*, **22**, 201–244.
Baxt,B. and Becker,Y. (1990) *Virus Genes*, **4**, 73–80.

Baxt,B., Morgan,D.O., Robertson,B.H. and Timpone,C.A. (1984) *J. Virol.*, **51**, 298–305.
Bittle,J.L., Houghten,R.A., Alexander,H., Shinnick,T.M., Sutcliffe,J.G., Lerner,R.A., Rowlands,D.J. and Brown,F. (1982) *Nature*, **298**, 30–33.
Borrego,B., Novella,I.S., Andreu,D., Giralt,E. and Domingo,E. (1993) *J. Virol.*, **67**, 6071–6079.
Brown,F. (1992) *Vaccine*, **10**, 1022–1026.
Brünger,A.T. (1992) *XPLOR Manual.* Version 3.0, Yale University, New Haven, CT.
Carreño,C., Roig,X., Cairó,J., Camarero,J., Mateu,M.G., Domingo,E., Giralt,E. and Andreu,D. (1992) *Int. J. Peptide Protein Res.*, **39**, 41–47.
Carrillo,C., Plana,J., Mascarella,R., Bergadá,J. and Sobrino,F. (1990) *Virology*, **179**, 890–892.
Case,D.A. and Karplus,M. (1979) *J. Mol. Biol.*, **132**, 343–368.
Clarke,B.E., Newton,S.E., Carroll,A.R., Francis,M.J., Appleyard,G., Syed,A.D., Highfield,P.E., Rowlands,D.J. and Brown,F. (1987) *Nature*, **330**, 381–384.
Compton,S.R., Nelsen,B. and Kirkegaard,K. (1991) *J. Virol.*, **64**, 4067–4075.
Connolly,M.L. (1983) *J. Appl. Crystallogr.*, **16**, 548–558.
Davies,D.R., Padlan,E.A. and Sheriff,S. (1990) *Annu. Rev. Biochem.*, **59**, 439–473.
Di Marchi,R., Brooke,G., Gale,C., Cracknell,V., Doel,T. and Mowat,N. (1986) *Science*, **232**, 639–641.
Díez,J., Mateu,M.G. and Domingo,E. (1989) *J. Gen. Virol.*, **70**, 3281–3289.
Dimmock,N.J. (1993) *Curr. Topics Microbiol. Immunol.*, **183**.
Domingo,E., Mateu,M.G., Martínez,M.A., Dopazo,J., Moya,A. and Sobrino,F. (1990) In Kurstak,E., Marusyk,R.G. and Murphy,B. (eds), *Applied Virology Research.* Plenum Press, New York, Vol. 2, pp. 233–266.
Domingo,E., Escarmís,C., Martínez,M.A., Martínez-Salas,E. and Mateu,M.G. (1992) *Curr. Topics Microbiol. Immunol.*, **176**, 33–47.
Domingo,E., Díez,J., Martínez,M.A., Martínez-Salas,E. and Mateu,M.G. (1993) *J. Gen. Virol.*, **74**, 2039–2045.
Fox,J., Parry,N., Barnett,P.V., McGinn,B., Rowlands,D.J. and Brown,F. (1989) *J. Gen. Virol.*, **70**, 625–637.
Furey,W. (1993) *PHASES Manual.* VA Medical Center, Pittsburg, PA.
Gebauer,F., de la Torre,J.C., Gomes,I., Mateu,M.G., Barahona,H., Tiraboschi,B., Bergmann,I., Augé de Mello,P. and Domingo,E. (1988) *J. Virol.*, **62**, 2041–2049.
Ghiara,J.B., Stura,E.A., Stanfield,R.L., Profy,A.T. and Wilson,I.A. (1994) *Science*, **264**, 82–85.
Hernández,J., Martínez,M.A., Rocha,E., Domingo,E. and Mateu,M.G (1992) *J. Gen. Virol.*, **73**, 213–216.
Holland,J.J., de la Torre,J.C. and Steinhauer,D.A. (1992) *Curr. Topics Microbiol. Immunol.*, **176**, 1–20.
Hynes,R.O. (1992) *Cell*, **69**, 11–25.
Kabsch,W. (1988) *J. Appl. Crystallogr.*, **21**, 916–924.
Kraulis,P.J. (1991) *J. Appl. Crystallogr.*, **24**, 946–950.
Krezel,A.M., Wagner,G., Seymour-Ulmer,J. and Lazarus,R.A. (1994) *Science*, **264**, 1944–1947.
Laskowski,R.A., MacArthur,M.W., Smith,D.K., Jones,D.T., Hutchinson,E.G., Morris,A.L., Naylor,D., Moss,D. and Thornton,J.M. (1994) *PROCHECK Manual.* Version 3.0, Oxford Molecular Ltd, Oxford, UK.
Laver,W.G., Air,G.M., Luo,M., Portner,A., Thompson,S.D. and Webster,R.G. (1990) In Laver,W.G. and Air,G. (eds), *Use of X-ray Crystallography in the Design of Antiviral Agents.* Academic Press, San Diego, CA, pp. 49–60.
Lazarus,R.A. and McDowell,R.S. (1993) *Curr. Opin. Struct. Biotechnol.*, **4**, 438–445.
Lea,S. *et al.* (1994) *Structure*, **2**, 123–139.
Leahy,D.J., Hendrickson,W.A., Aukhil,I. and Erickson,H.P. (1992) *Science*, **258**, 987–991.
Logan,D. *et al.* (1993) *Nature*, **347**, 566–568.
Martínez,M.A., Hernandez,J., Piccone,M.E., Palma,E.L., Domingo,E., Knowles,N. and Mateu,M.G. (1991a) *Virology*, **184**, 695–706.
Martínez,M.A., Carrillo,C., Gonzalez-Candelas,A., Moya,A., Domingo,E. and Sobrino,F. (1991b) *J. Virol.*, **65**, 3954–3957.
Mason,P.W., Rieder,E. and Baxt,B. (1994) *Proc. Natl Acad. Sci. USA*, **91**, 1932–1936.
Mateu,M.G. *et al.* (1987) *Virus Res.*, **8**, 261–274.
Mateu,M.G., Martínez,M.A., Rocha,E., Andreu,D., Parejo,J., Giralt,E., Sobrino,F. and Domingo,E. (1989) *Proc. Natl Acad. Sci. USA*, **86**, 5883–5887.
Mateu,M.G., Martínez,M.A., Capucci,L., Andreu,D., Giralt,E., Sobrino,F., Brocchi,E. and Domingo,E. (1990) *J. Gen. Virol.*, **71**, 629–637.
Mateu,M.G., Andreu,D., Carreño,C., Roig,X., Cairó,J.-J., Camarero,J.A., Giralt,E. and Domingo,E. (1992) *Eur. J. Immunol.*, **22**, 1385–1389.
Mateu,M.G. *et al.* (1994) *J. Virol.*, **68**, 1407–1417.
Navaza,J. (1994) *Acta Crystallogr.*, **A50**, 157–163.
Novella,I.S., Borrego,B., Mateu,M.G., Domingo,E., Giralt,E. and Andreu,D. (1993) *FEBS Lett.*, **330**, 253–259.
Olson,N.H., Kolatkar,P.R., Oliveira,M.A., Cheng,R.H., Greve,J.M., McClelland,A., Baker,T.S. and Rossmann,M.G. (1993) *Proc. Natl Acad. Sci. USA*, **90**, 507–511.
Parry,N., Fox,G., Rowlands,D., Brown,F., Fry,E., Acharaya,R., Logan,D. and Stuart,D. (1990) *Nature*, **347**, 569–572.
Pereira,H.G. (1981) In Gibbs,E.P. (ed.), *Virus Diseases of Food Animals.* Academic Press, London, UK, pp. 333–363.
Pfaff,E., Mussgay,M., Bohm,H.O., Schulz,G.E. and Schaller,H. (1982) *EMBO J.*, **1**, 869–874.
Reynolds,C., Page,G., Zhou,H. and Chow,M. (1991) *Virology*, **184**, 391–396.
Rini,J.M., Schulze-Gahmen,U. and Wilson,I.A. (1992) *Science*, **255**, 959–965.
Rossmann,M.G. (1989) *J. Biol. Chem.*, **264**, 14587–14590.
Rossmann,M.G. *et al.* (1985) *Nature*, **317**, 145–153.
Rousel,A. and Cambillau,C. (1991) *TURBO Manual.* Silicon Graphics, Mountain View, CA.
Rowlands,D.J., Clarke,B.E., Carroll,A.R., Brown,F., Nicholson,B.H., Bittle,J.L., Houghten,R.A. and Lerner,R.A. (1983) *Nature*, **306**, 694–697.
Ruoslahti,E. (1988) *Annu. Rev. Biochem.*, **57**, 375–413.
Smith,T.J. *et al.* (1993) *J. Virol.*, **67**, 1148–1158.
Steinhauer,D. and Holland,J.J. (1987) *Annu. Rev. Microbiol.*, **41**, 409–433.
Strohmaier,K., Franze,R. and Adam,K.H. (1982) *J. Gen. Virol.*, **59**, 295–306.
Surovoi,A.Y., Ivanov,V.T., Chepurkin,A.V., Ivanyuschenkov,V.N. and Dryagalin,N.N. (1989) *Sov. J. Bioorg. Chem.*, **14**, 527–580.
Tormo,J., Blas,D., Parry,N.R., Rowlands,D., Stuart,D. and Fita,I. (1994) *EMBO J.*, **13**, 2247–2256.
Tulip,W.R., Varghese,J.N., Webster,R.G., Laver,W.G. and Colman,J. (1992) *J. Mol. Biol.*, **227**, 149–159.
Verdaguer,N., Mateu,M.G., Bravo,J., Tormo,J., Giralt,E., Andreu,D., Domingo,E. and Fita,I. (1994) *Proteins*, **18**, 201–203.
Webster,D.M., Henry,A.H. and Rees,A.R. (1994) *Curr. Opin. Struct. Biol.*, **4**, 123–129.
Wilson,I.A. and Stanfield,R.L. (1993) *Curr. Opin. Struct. Biol.*, **3**, 113–118.
Wistow,G., Turnell,B., Summers,L., Slingsby,C., Moss,D., Miller,L., Lindley,P. and Blundell,T. (1983) *J. Mol. Biol.*, **170**, 175–202.

Received on November 4, 1994; revised on December 21, 1994